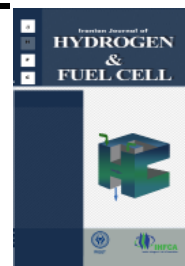


Iranian Journal of Hydrogen & Fuel Cell

**IJHFC**

Journal homepage://ijhfc.irost.ir



## **Electrochemical impedance spectroscopy for investigation of different losses in 4-cells short stack with integrated humidifier and water separator**

**E. Alizadeh\*, M. Khorshidian\*\*, S. M. Rahgoshay, S. H. M. Saadat, M. Rahimi-Esbo**

Fuel Cell Technology Research Laboratory, Malek Ashtar University of Technology, Fridonkenar, Islamic Republic of Iran

### **Article Information**

Article History:

Received:

09 July 2016

Received in revised form:

05 Oct 2016

Accepted:

19 Oct 2016

### **Keywords**

PEM Fuel Cell (PEMFC)

Cascade type stack

Electrochemical Impedance Spectroscopy (EIS)

Dead-end Operation

### **Abstract**

Electrochemical impedance spectroscopy (EIS) is a suitable and powerful diagnostic testing method for fuel cells (FCs) since it is non-destructive and provides useful information about FC performance and its components. In this study, a 500W cascade type 4 cells stack with integrated humidifier, water separator and internal manifolds was designed, fabricated and tested for the first time. The diagnostic test was conducted by EIS. The effects of dead end and open end modes of the stack impedance spectra are studied. The results suggested that ohmic resistance of the single cell decreased as the current density increased due to the greater effect of hydration of membrane. The results of the electrochemical impedance revealed that the gas operating mode had significant impact on electrochemical impedance of the stack. When the stack was tested on dead end mode, the charge transfer resistance of the stack decreased dramatically and its influence on mass transfer resistances was negligible.

## **1. Introduction**

Fuel cell technology has been significantly developed in comparison with other power generators due to its unique energy conversion characteristics. Compared to various other types of FCs, it seems that proton

exchange membrane fuel cells (PEMFCs) are a suitable choice for stationary and portable applications due to their high energy conversion, low operating temperatures, high power density production, quiet operating condition, quick startup up and shutdown, and ultimately eco-friendly features [1-4]. However, obstacles such as reliability, endurance, and cost impede the commercialization of PEMFCs. That is

\*Corresponding Author's Fax: +981135665090

E-mail address: [fccenter@mut.ac.ir](mailto:fccenter@mut.ac.ir)

\*\*Corresponding Author's Fax: +981135665090

E-mail address: [khorshidian@mut.ac.ir](mailto:khorshidian@mut.ac.ir)

why PEMFC applications are restricted to research and demonstration applications [2]. Fundamental experimental investigations of single cell PEMFC have been recently conducted, but stack-level investigations have received less attention.

The performance of PEMFC should be checked by various testing techniques to evaluate new materials, to validate new designs, to assess new experimental techniques, and to optimize operating procedures. Testing techniques is a constant companion to any set of diagnostic tools, so that the results can be viewed in the proper context. There are several methods for diagnosing and analyzing PEMFCs. These methods are usually divided into two main groups: physical/chemical tests such as gas chromatography (GC), pressure drop measurement, and magnetic resonance imaging (MRI) [1-3]; and electrochemical tests such as voltammetry sweep, current interruption, and electrochemical impedance spectroscopy (EIS) [1-4].

EIS has been demonstrated to be a powerful experimental technique to examine the complexity of the different processes taking place in fuel cells. This method is non-destructive and provides useful information about FC performance and its components without disturbing it from equilibrium state. The main advantage of the EIS is its ability to distinguish between the individual contributions of the interfacial charge transfer and the mass transport resistances in the catalyst layer and diffusion layer. On the other hand, this approach does not generate local information [2].

EIS can be utilized to optimize properties of the membrane electrode assembly (MEA) [6-8]. EIS has also been applied to measure the ohmic resistance of the FC [9-10], to optimize the FC operating conditions [11-13], and to investigate the effect of contamination [14-16]. Even though much effort has been made to diagnose the PEMFC performance by applying EIS, most of these studies have concentrated on single cells with small or partially medium active areas [17]. Basically, large active areas result in higher current densities making it necessary to use a high power test station and a high-duty load bank

without an appropriate frequency response which adds significant complexity to the measurement set-up. In addition, only a limited amount of work has been done with PEMFC stacks, especially with large active areas [2, 17 and 18].

Giner-Sanz et al. [19] studied the optimum impedance measurement parameters, such as second integration time, integration cycles, stabilization cycles, second maximum tabilization time and a minimal fraction, for the system. Furthermore, they highlighted the importance of proper selection of impedance measurement parameters. They recommended that optimization of the measurement parameters should be performed for each particular system instead of the general practice of taking the default measurement parameter values.

Zhiani et al. [20] demonstrated that membrane electrode assembly (MEA) conditioning at the low stress condition produces a higher performance compared to MEA conditioning at the high stress condition, although it needs more time to accomplish. They reported MEA conditioning at the low stress condition enhanced not only the fuel cell power but also its energy efficiency by 25%. They compared electrochemical impedance spectroscopy (EIS) responses of MEA-LTP and MEA-HTP and showed that an extension of the triple phase boundary occurred in MEA-LTP, which was consistent with the results of the MEA performance analysis.

Asghari et al. [21] used electrochemical impedance spectroscopy to examine the effect of working conditions on the performance of a self-humidified dead-ended anode fuel cell. Their results showed that the performance was enhanced by increasing the working temperature up to 50 °C, but further increase of the temperature caused an intense reduction in the performance due to a combination of severe membrane drying and build-up of nitrogen in the anode side. They reported impedance spectra were greatly influenced by the air stoichiometry since increasing the air stoichiometry might lead to severe membrane drying on one hand, and increasing mass transport resistance due to accumulation of N<sub>2</sub> in the anode side on the other hand. They reported

that the impedance spectra were greatly influenced by the air stoichiometry since increasing the air stoichiometry might lead to severe membrane drying on one hand, and increasing mass transport resistance due to accumulation of  $N_2$  in the anode side on the other hand. They reported that the impedance spectra were less affected by the purge interval at its low values, and large values of the purge interval led to significant mass transport issues.

Barzegari et al. [22] investigated the effect of temperature on the performance of a dead-end cascade  $H_2/O_2$  polymer electrolyte membrane (PEM) fuel cell stack. The PEMFC stack, humidifier and separator were modeled mathematically. They considered a cascade stack with two stages to use almost all reactant gases during operation. They reported the obtained model simply presents the behavior of dead-end PEMFC, which can then be used for identification and control purposes.

In a dead-end design utilization of reactant gases is complete. In this system, the intensive water accumulation causes flooding in the gas diffusion layer. This unfavorable phenomenon can lead to local fuel starvation and subsequently increases mass transfer resistance of the three phase/s interface, which deteriorates the performance and durability of PEMFCs. In this paper, a new design for a PEMFC stack is used. The basic concept of the proposed design is to divide the cells of a stack into two blocks by transporting the outlet gas of each stage to a separator and re-introducing it in the next stage. There are only a few papers which used EIS for investigation of voltage losses in a dead-end PEMFC stack. In this study, a cascade type stack with integrated humidifier and water separator and internal manifolds was designed, fabricated and tested for the first time. The advantage of the dead-end design compared to an open-end one is investigated by EIS. In this test, the impedance spectra of each cell and the stack are plotted simultaneously. The previous studies did not pay adequate attention to the investigation of voltage losses in the PEMFC stack. The effect of increasing current density on the dead-end cascade FC is analyzed and the resistances

resulting from impedance are investigated.

## 2. Experimental investigation

### 2.1. PEM fuel-cell stack design, fabrication and testing

Fig. 1 shows a schematic drawing of the proposed design for a PEMFC stack which is not equipped with any hydrogen or oxygen recirculation devices. The integrated separators were used to remove liquid water from the mixture of hydrogen, oxygen and water exiting each stage. An applied unified humidifier is used to increase the humidity at the entrance of the stack as well as decreasing the size of the stack by reducing external devices. Fig. 2 shows the fabricated 4-cells PEMFC short stack and its related equipment.

The 500 W short stack consisted of four cells with an active area of  $225 \text{ cm}^2$ . The MEAs consisted of nafion 112 membranes, catalyst layers with a total Pt loading of  $0.4 \text{ mg cm}^2$  at the anode side and Pt/Pd loading of  $0.4 \text{ mg cm}^2$  at the cathode side, and SGL carbon cloth with a microporous layer as the gas diffusion layers (GDLs). The anode and cathode flow fields have a parallel serpentine pattern.

The experiments were conducted using a 5 kW test station with a FC impedance meter (KFM2150, Kikusui Electronics, Japan) in a galvanostatic mode. The advantage of using the KFM2150 impedance meter is that the impedance of the stack was measured when the impedance of all cells were measured. The hydrogen and oxygen gases were humidified by an internal membrane gas humidifier.

The impedance spectra were recorded by sweeping frequencies in the range of 0.1 Hz to 10 kHz. The amplitude of the AC signal was 10% of the DC current magnitude. At the relative humidity higher than 85%, the hydrogen and oxygen gases were discharged at a constant stoichiometry of 1.003 and 1.010, respectively. Operating temperature of the short stack was kept constant at  $70 \text{ }^\circ\text{C}$ .

### 2.2. Electrical model of the FC

The Nyquist plot is the most common way of analyzing impedance data. Generally, Nyquist plots may include

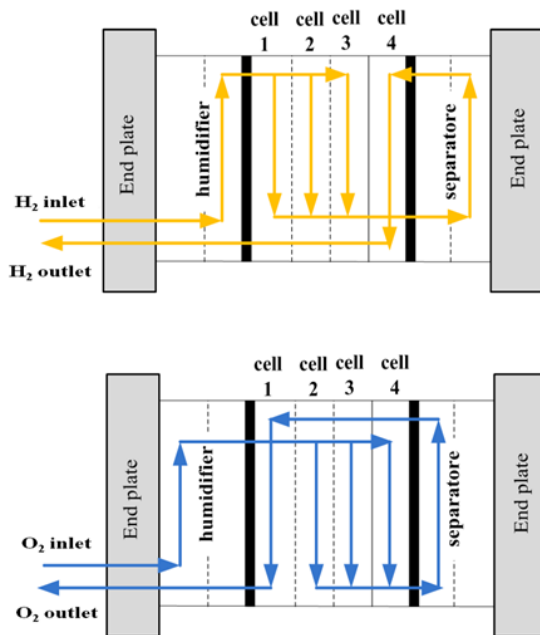


**Fig. 1. Schematic illustration of the proposed PEMFC stack design.**

one, two, or three arcs: the impedance loops in the Nyquist plot are described as high, medium, and low frequency loops, respectively. These loops can be attributed to the structural features of the MEA, charge transfer resistance with double layer capacitance of the catalyst layer, and mass transfer resistance [17]. The fuel cell can be modeled by the equivalent circuit shown in Fig. 3. The anodic polarization is very small and can be neglected. Thus, the obtained impedance spectrum mainly reflects the cathode polarization; the associated elements of the anode can be omitted.  $R_{\Omega}$  (intersection with the real axis in the impedance spectrum) is the high-frequency resistance (HFR) representing the ohmic resistance of the stack;  $R_{ct}$  is the charge transfer resistance due to the oxygen reduction reaction (ORR);  $R_{mt}$  is the resistance related to the mass transport of  $O_2$  in both the catalyst layer and the GDL; and CPE is the constant phase element capacitance properties [12]. For a better understanding of the electrochemical processes involved in the operation of the 4-cells short stack, an equivalent circuit has been set up based on the characteristics of FC reactions and the measured impedance spectra of the mentioned stack (Fig. 3). The measured electrochemical impedance spectra were fitted using EIS spectrum analyzer software.

The AC impedance spectrum and its fitting curve are illustrated in Fig. 4. The curve properly fits the obtained responses; hence, the electrochemical processes of the stack can be analyzed by the equivalent circuit.

### 3. Result and discussion

#### 3.1. Effect of output current

Firstly, the stack was conditioned according to the PaxiTech Company conditioning procedure for a period of time before measuring its performance. Stacks are more likely to encounter more defects than single cells. These defects aren't found easily by conventional methods and their diagnoses need more effective techniques such as the EIS method. In this work, all of

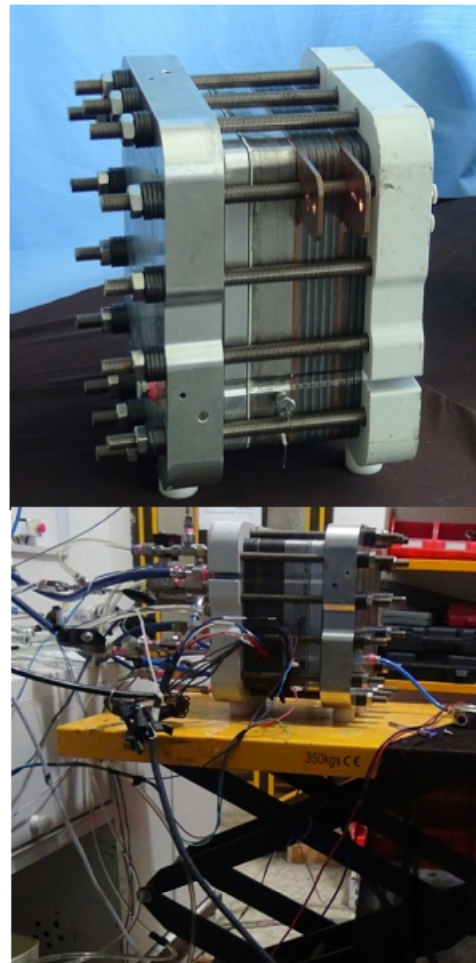


**Fig. 2. Dead-end stack with liquid separators, humidifiers and cell voltage monitoring cables.**

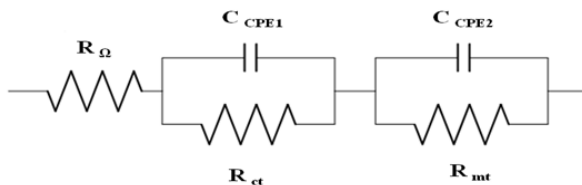


Fig. 3. Equivalent circuit for impedance analysis on the FC stack [17].

the parameters affecting the performance of the short stack were considered constant except for the current density which is in the range of 100 to 500 mA cm<sup>-2</sup>.

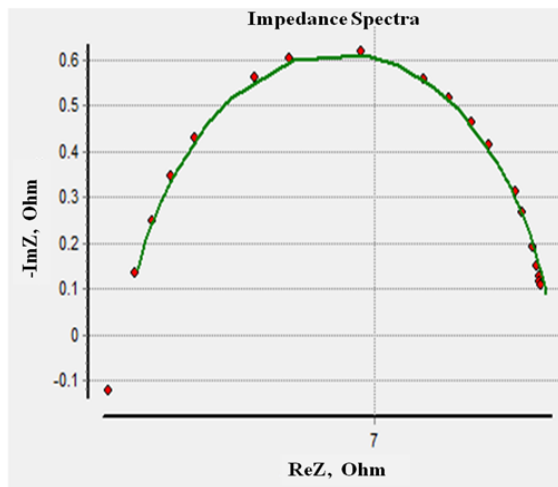


Fig. 4. AC impedance spectra and its fitting curve for the 4-cells short stack at 135A.

### 3.2. Dead end mode

The impacts of the output current changes on the impedance spectroscopy and their corresponding performance curves are shown in Figs. 5 and 6. Fig. 5 illustrates that the kinetic loop diameter reduces as the current density increases revealing the decrement of the charge transfer resistance. The driving force for the oxygen reduction reaction gradually increases as the the output current increases. Therefore, the charge transfer resistance of the single cell gradually decreases. It was expected that the change of HFR with increasing current density would be slight or negligible, but the high frequency intercept part experienced considerably changes with the changes of output current (Fig. 5). Indeed, this change is complicated and affected

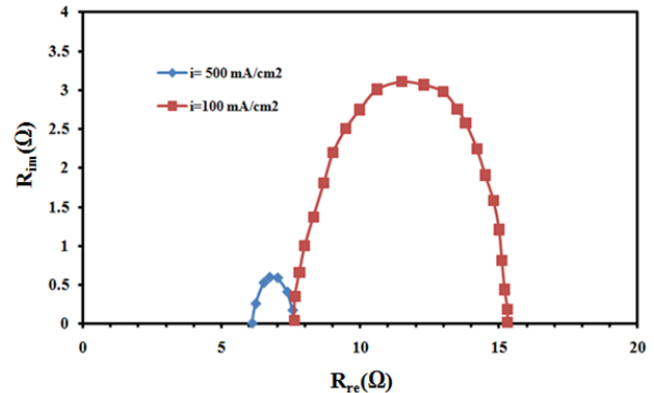


Fig. 5. AC impedance spectra of the 4-cells short stack with different output current densities at dead-end mode ( $T=70^{\circ}\text{C}$ ; solid line:  $i=500\text{ mA/cm}^2$ , dashed line:  $i=100\text{ mA/cm}^2$ ).

by many factors such as the water content of the membrane and the contact resistance. The contact resistance includes the contact resistances between the membrane/electrode, electrode/bipolar plate, bipolar plate/bipolar plate and end bipolar plate/current collector plate, which are shown in Fig. 7.

It should be noted that the times for opening and closing the purge solenoid valve are 2 s and 4 s for cathodic cells and 2 s and 6 s for anodic cells.

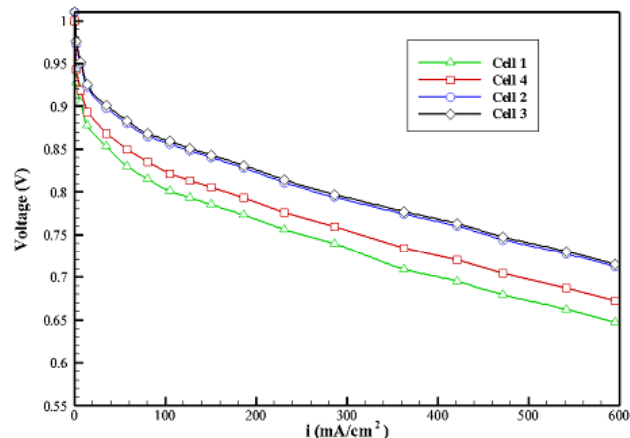


Fig. 6. The polarization curve of the 4-cells short stack at  $70^{\circ}\text{C}$  operating temperature.

According to the notable difference of HFR at the current densities in the range of 100 to 500 mA/cm<sup>2</sup>, the Nyquist diagram of each single cell was used. One of the important priorities in our test was to use a Kikusui impedance meter because it has the ability to

measure the electrochemical impedance of each cell and the stacks, simultaneously. The electrochemical impedance spectra of each single cell in two different current densities are shown in Fig. 8.

It should be noted that at dead-ended mode operation, the voltages are not constant and drop until the purge valve opens. However, one of the prerequisites of the EIS method is stable and constant operating conditions and voltages during impedance measurements.

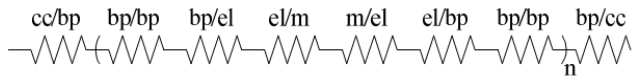


Fig. 7. Contact resistance of the stack parts (n represents the number of cells in the stack).

To solve this issue the number of impedance measurement moving average is set on number 8 which curbed the effect of voltage variation during the test.

The ohmic resistances of cells in the oxygen first stage (cell number 2, 3, and 4) are approximately equal, while the ohmic resistance of cell 1 is higher than the others at  $i=100 \text{ mA/cm}^2$  (Fig. 8a). The oxygen stoichiometry of the first and the second stage are 1.3 and 1, respectively. As a result, the water content of the membrane in the first stage of oxygen is higher than the second stage, and the ohmic resistance of cell 1 is higher than the others. The generated water increases by enhancing the current density and the hydration level of the membrane. Consequently, the ohmic resistance decreases slightly in cells 2, 3 and 4. Indeed, the ohmic resistance of cell 1 decreases dramatically, which is attributed to the similar hydration level of this cell to the first stage cells (Fig. 8b).

The changes in HFR,  $R_{mt}$ ,  $R_{ct}$  of each cell at output current density of 100 and 500  $\text{mA/cm}^2$  obtained from the proposed equivalent electrical model (Fig. 3) are shown in Fig. 9. At low current density (Fig. 9a), the reduction rate of oxygen, denoted by the charge transfer resistance ( $R_{ct}$ ), is high. Moreover, the  $\text{O}_2$  mass transfer resistance to reaction interface increased by the enhancement of current density.

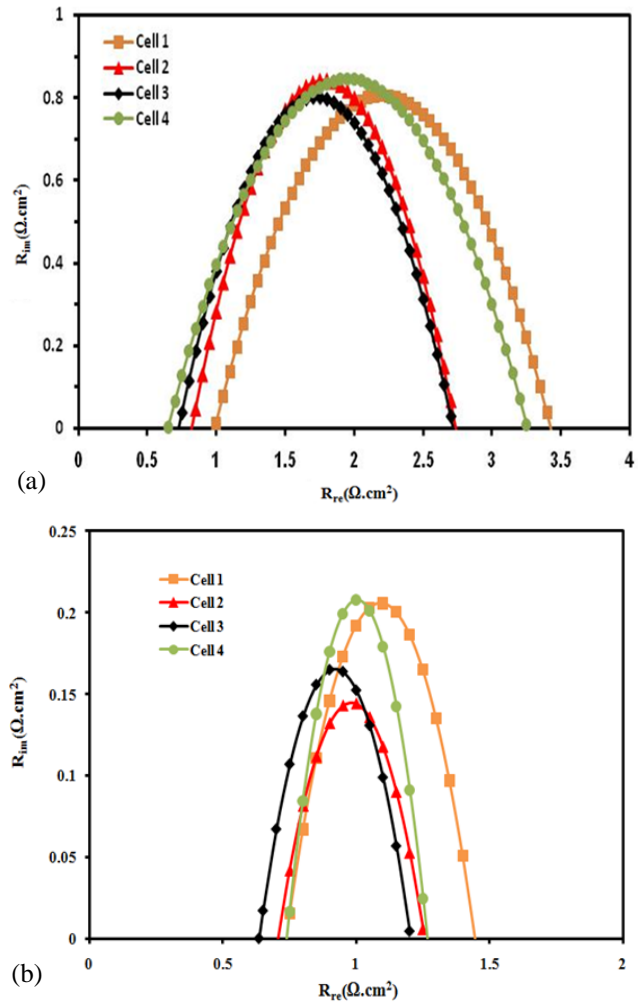


Fig. 8. AC impedance spectra of the each single cell at output current densities a) 100 and b) 500  $\text{mA/cm}^2$  at the operating temperature of 70 °C.

### 3.3. Open end mode

Uncompleted utilization of reactant gases in the open-end mode lead to higher stoichiometry of reactant gases than the dead-end mode. Hydrogen and oxygen were fed to the stack at a constant stoichiometry of 1.2 and 1.5, respectively. In this case, the inlet relative humidity and the operating temperature of the short stack were kept at 85% and 70 °C, respectively. The impedance spectra, recorded by sweeping frequencies over the range of 10 kHz to 0.1 Hz, suggest that the amplitude of the AC signal was 10% of the DC current magnitude. Fig. 10 shows the polarization curve at different

operating modes. The losses become more significant as the current density increases due to hydrogen and oxygen mass transfer resistance (Fig. 10). The frequency impedance plots of the 4-cells short stack at different operating modes are shown in Fig. 11.

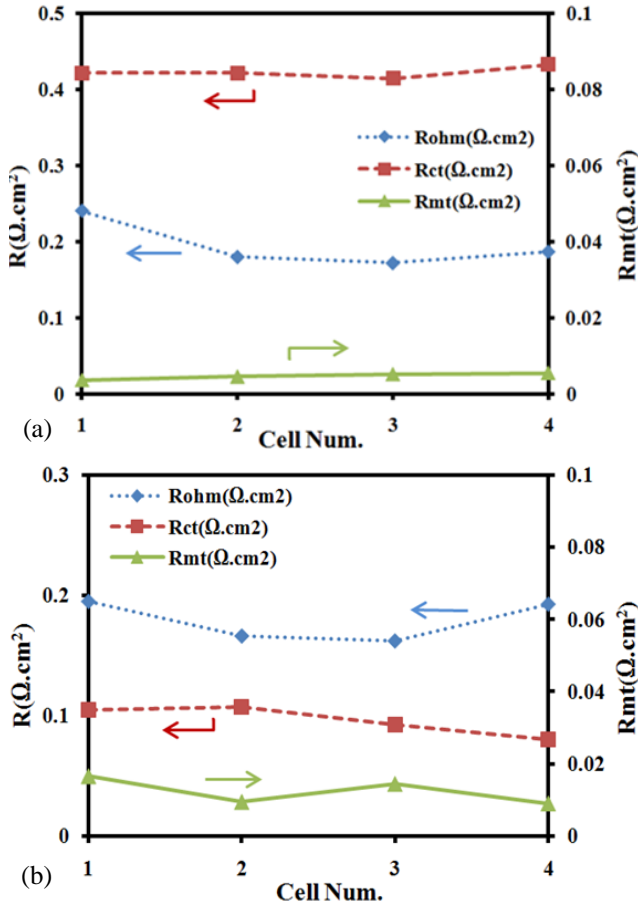


Fig. 9. The dependence of the ohmic resistance ( $R_{ohm}$ ), the charge transfer resistance ( $R_{ct}$ ) and the mass transport resistance ( $R_{mt}$ ) of the each single cell with a)  $i=100 \text{ mA/cm}^2$  and b)  $i=500 \text{ mA/cm}^2$  ( $T=70^\circ\text{C}$ ).

The HFR decreases due to higher stoichiometry of humidified gases and better membranes proton conductivity when PEMFC operates at an open-end mode. The prominent point in the Nyquist diagram is the charge transfer increment caused by the open-ended mode. These complicated phenomena can be easily inspected by single cell impedance plots. The electrochemical impedance spectra of each single cell (at  $i=500 \text{ mA/cm}^2$ ) at the open-end mode are shown in Fig. 12.

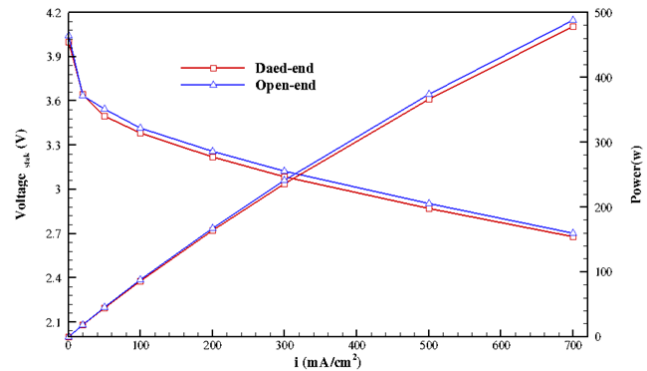


Fig. 10. The performance curve of the short stack at different reactant flowing mode (the operating temperature was  $70^\circ\text{C}$ ). (Inside the graph, change Daed-end to Dead-end).

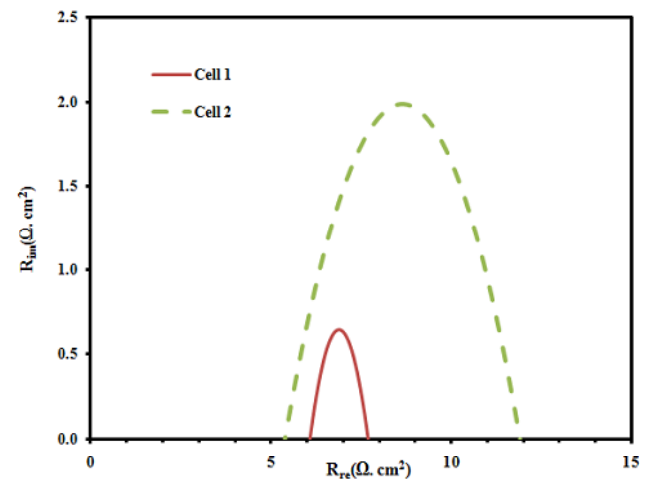


Fig. 11. AC impedance spectra of the 4-cells short stack at different operating modes ( $i=500 \text{ mA/cm}^2$ ,  $T=70^\circ\text{C}$ ) (DE and OE represent dead-end and open-end mode, respectively).

Fig. 13a illustrates the ohmic resistances of all cells in an open-end mode which are approximately equal and lower than the same cells in the dead-end mode. This reduction is related to the higher reactant flow rate and increased water content of the membrane. By increasing the water content of the membrane, its protonic conductivity increases; contrarily, the HFR decreases.

The mass transport resistance in cell 1 is higher than cell 2, and cell 2 is higher than cells 3 and 4 (Fig. 13a). An increase in the hydrogen stoichiometry at the open-end mode as well as the cascade type of the short stack manifold would result in a lower flow

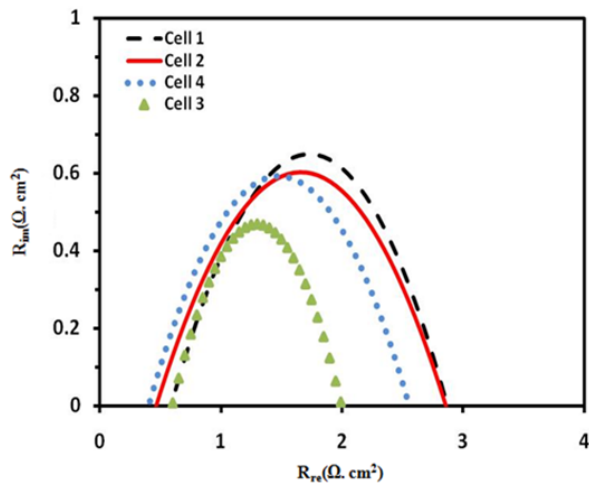


Fig. 12. AC impedance spectra of the each single cell at the open-end mode ( $i=500\text{ mA/cm}^2$ ,  $T=70^\circ\text{C}$ ).

rate of hydrogen in cell 1 than cells 2 and 3 (see Fig. 1). As a result, higher mass transport resistance tends to cause an adverse effect. It should be mentioned that the stoichiometry of hydrogen in cell 4 at the hydrogen second stage was approximately 3, which explains the extra hydrogen for oxidation. Therefore, the mass transport limitation was very low as illustrated in Fig. 13a. On the other hand, cell 2 is the first cell of the early stage of oxygen (see Fig. 1) and due to the inlet effect faces more oxygen mass transport limitation compared to cells 3 and 4, which are in the first stage of oxygen.

#### 4. Conclusions

In this study, the performance of a PEMFC short stack with an integrated humidifier and water separator is investigated by the EIS approach. A new cascade type design with two stages was used for the stacks. The basic concept of the proposed design was to divide the cells of a stack into two blocks; hence, the stoichiometry of the first stage of hydrogen and oxygen was more than 1.3. This design helped to prevent water flooding at the first stage. The effects of the operating mode and the current density were meticulously investigated. The results of the electrochemical impedance suggested that the gas operating mode had major effects on the

electrochemical impedance of the stack. When the stack was tested in the dead-end mode, the charge transfer resistance of the stack decreased significantly. In addition, this mode only slightly affected the mass transfer resistances. Moreover, the current density played an important role in the electrochemical impedance in the dead-end mode. The ohmic resistance of the single cells decreased by increasing the current density due to increased hydration of the membranes. Moreover, higher ORR would lead to a gradual decrease in the charge transfer resistance of the stack at higher current density. The AC impedance diagnosis of the stack could provide researchers with some useful information about the

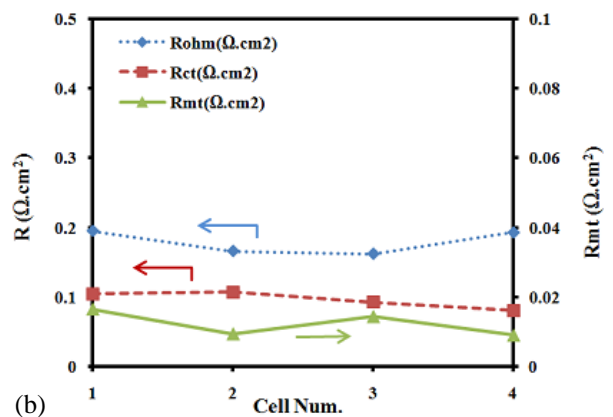
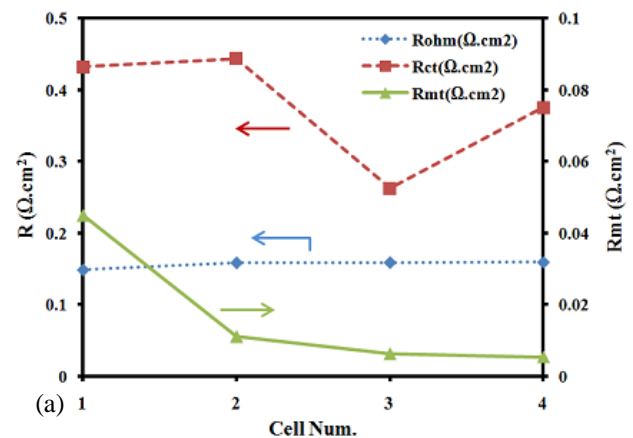


Fig. 13. The dependence of the ohmic ( $R_{oh}$ ), charge transfer ( $R_{ct}$ ) and the mass transport resistance ( $R_{mt}$ ) of the each single cell in a) open-end mode and b) dead-end mode ( $i=500\text{ mA/cm}^2$ ,  $T=70^\circ\text{C}$ ).

FC stack, especially in a dead-end cascade type stack whose mode evaluation is more complicated.

## 5. References

- [1] Wang H., Yuan X., Li H., "PEM Fuel Cell Diagnostic Tools", CRC Press, 2012.
- [2] Yuan X., Sun J.C., Wang H., Zhang J., "AC impedance diagnosis of a 500WPEM fuel cell stack: part II: individual cell impedance", J. Power Sources, 2006, 161: 929.
- [3] Wu J., Zi Yuan X., Wang H., Blanco M., Martin J.J., Zhang J., "Diagnostic tools in PEM fuel cell research: part II: physical/chemical methods", Int. J. Hydrogen Energy, 2008, 33: 1747.
- [4] Wu J., Yuan X.Z., Wang H., Blanco M., Martin J.J., Zhang J., "Diagnostic tools in PEM fuel cell research: part I electrochemical techniques", Int. J. Hydrogen Energy, 2008, 33: 1735.
- [5] Millera M., Bazylaka A., "A review of polymer electrolyte membrane fuel cell stack testing", J. Power Sources, 2011, 196: 601.
- [6] Wagner N., Kaz T., Friedrich K.A., "Investigation of electrode composition of polymer fuel cells by electrochemical impedance spectroscopy", J. Electrochim. Acta, 2008, 53: 7475.
- [7] Easton E.B. and Pickup P.G. "An electrochemical impedance spectroscopy study of fuel cell electrodes", J. Electrochim Acta, 2005, 50: 2469.
- [8] Guo Q., Cayetano M., Tsou Y., DeCastro E., White R., "Study of ionic conductivity profiles of the air cathode of a PEMFC by AC impedance spectroscopy", J. Electrochem Soc, 2003, 150: 1440.
- [9] Makharia R., Mathias M., Baker D., "Measurement of catalyst layer electrolyte resistance in PEFCs using electrochemical impedance spectroscopy", J. Electrochem. Soc, 2005, 152: 970.
- [10] Easton E., Astill T., Holdcroft S., "Properties of gas diffusion electrodes containing sulfonated poly (ether ether ketone)", J. Electrochem. Soc, 2005, 152: 752.
- [11] O'Rourke J., Ramani M., Arcak M., "Using electrochemical impedance to determine airflow rates", Int. J. Hydrogen Energy, 2008, 33: 4694.
- [12] Roy S. and Orazem M., "Analysis of flooding as a stochastic process in polymer electrolyte membrane (PEM) fuel cells by impedance techniques", J. Power Sources, 2008, 184: 212.
- [13] Brunetto C., Moschetto A., Tina G. PEM fuel cell testing by electrochemical impedance spectroscopy. Elec Power Syst Res 2009, 79:17-26.
- [14] Wagner N. and Gu' lzw E., "Change of electrochemical impedance spectra (EIS) with time during CO-poisoning of the Pt-anode in a membrane fuel cell", J. Power Sources, 2004, 127: 341.
- [15] Yang D., Ma J., Xu L., Wu M., Wang H., "The effect of nitrogen oxides in air on the performance of proton exchange membrane fuel cell", J. Electrochim. Acta, 2006, 51: 4039.
- [16] Li H., Zhang J., Fatih K., Wang Z., Tang Y., Shi Z., "Polymer electrolyte membrane fuel cell contamination: testing and diagnosis of toluene-induced cathode degradation", J. Power Sources, 2008, 185: 272.
- [17] Yuan X., Sun J.C., Blanco M., Wang H., Zhang J., Wilkinson D.P., "AC impedance diagnosis of a 500WPEM fuel cell stack: part I: stack impedance", J. Power Sources, 2006, 161: 920.
- [18] Zhu W.H., Payne R.U., Tatarchuk B.J, "PEM stack test and analysis in a power system at operational load via ac impedance", J. Power Sources, 2007, 168: 211.
- [19] Giner-Sanz, J.J., Ortega, E.M., Pérez-Herranz, V. Optimization of the electrochemical impedance spectroscopy measurement parameters for PEM fuel cell spectrum determination, Electrochimica Acta 174, 2015, 1290–1298.

[20] Zhiania, M., Majidi, S., Bruno Silva, V., Gharibi, H. Comparison of the performance and EIS (electrochemical impedance spectroscopy) response of an activated PEMFC (proton exchange membrane fuel cell) under low and high thermal and pressure stresses, *Energy* 97, 2016, 560-567.

[21] Asghari, S., Ashraf Khorasani, M., Dashti, R. I. Investigation of self-humidified and dead-ended anode proton exchange membrane fuel cell performance using electrochemical impedance spectroscopy, *International Journal of Hydrogen Energy*, 41, 2016, 12347-12357.

[22] Barzegari, M., M. Dardel, M., Ramiar, A., Alizadeh, E. An investigation of temperature effect on performance of dead-end cascade H<sub>2</sub>/O<sub>2</sub>PEMFC stack with integrated humidifier and separator, *International Journal of Hydrogen Energy*, 41, 2016, 3136-3146.